Stem Cell Reports
Article

OPEN ACCESS

The PAF1c Subunit CDC73 Is Required for Mouse Hematopoietic Stem Cell Maintenance but Displays Leukemia-Specific Gene Regulation

Nirmalya Saha,[1] James Ropa,[1,2] Lili Chen,[1] Hsiangyu Hu,[1] Maria Mysliwski,[1] Ann Friedman,[3] Ivan Maillard,[3,4] and Andrew G. Muntean[1,*]

[1]Department of Pathology, University of Michigan Medical School, 7520B Medical Science Research Building I, 1150 W. Medical Center Dr., Ann Arbor, MI 48109-5602, USA

[2]Department of Computational Medicine and Bioinformatics, University of Michigan Medical School, Ann Arbor, MI 48109, USA

[3]Life Sciences Institute, University of Michigan, Ann Arbor, MI 48109, USA

[4]Division of Hematology-Oncology, Department of Medicine and Abramson Family Cancer Research Institute, University of Pennsylvania Perelman School of Medicine, Philadelphia, PA 19104, USA

*Correspondence: andrewmu@umich.edu

https://doi.org/10.1016/j.stemcr.2019.03.010

SUMMARY

The Polymerase Associated Factor 1 complex (PAF1c) functions at the interface of epigenetics and gene transcription. The PAF1c is required for MLL fusion-driven acute myeloid leukemia (AML) through direct regulation of pro-leukemic target genes such as *Hoxa9* and *Meis1*. However, the role of the PAF1c in normal hematopoiesis is unknown. Here, we discovered that the PAF1c subunit, CDC73, is required for both fetal and adult hematopoiesis. Loss of *Cdc73* in hematopoietic cells is lethal because of extensive bone marrow failure. *Cdc73* has an essential cell-autonomous role for adult hematopoietic stem cell function *in vivo*, and deletion of *Cdc73* results in cell-cycle defects in hematopoietic progenitors. Gene expression profiling indicated a differential regulation of *Hoxa9*/*Meis1* gene programs by CDC73 in progenitors compared with AML cells, suggesting disease-specific functions. Thus, the PAF1c subunit, CDC73 is essential for hematopoietic stem cell function but exhibits leukemia-specific regulation of self-renewal gene programs in AML cells.

INTRODUCTION

Epigenetic pathways play an important role in hematopoietic development and are frequently dysregulated in acute leukemias (Cancer Genome Atlas Research Network et al., 2013). This illustrates the importance of proper epigenetic regulation for normal hematopoietic development. The Polymerase Associated Factor 1 complex (PAF1c) is an epigenetic regulator complex functioning at the intersection of transcription and epigenetics. The PAF1c consists of six subunits, including PAF1, RTF1, CTR9, LEO1, CDC73, and WDR61, several of which are implicated in solid tumor progression through mutation or overexpression (Carpten et al., 2002; Hanks et al., 2014; Moniaux et al., 2006; Mueller and Jaehning, 2002; Wade et al., 1996; Zeng and Xu, 2015). We and others have shown that the PAF1c is essential for several subtypes of acute myeloid leukemia (AML), including those with *MLL1* (*KMT2a*) translocations (Milne et al., 2010; Muntean et al., 2010, 2013).

The PAF1c binds directly to RNA polymerase II through the CDC73, PAF1, and LEO1 subunits (Xu et al., 2017). It is involved in multiple stages of metazoan transcription, including transcription initiation, elongation, termination, and mRNA processing (Jaehning, 2010; Tomson and Arndt, 2013; Van Oss et al., 2017). Several lines of evidence suggest that PAF1c is associated with chromatin regions undergoing active transcription; however, only a subset of these genes is regulated by this complex (He et al., 2011; Kim et al., 2004; Pavri et al., 2006; Qiu et al., 2006; Yu et al., 2015). However, accumulating data also suggest a context-dependent role of PAF1c in gene repression (Mueller et al., 2006). For example, the PAF1c was shown to facilitate promoter proximal pausing by localizing to transcriptional enhancers to block hyperactivation of a specific subset of genes (Chen et al., 2015, 2017). In addition, the PAF1c plays a role in transcriptional activation by functioning as a bridge to connect epigenetic modifying factors to chromatin. For instance, through protein interactions with PAF1 and RTF1, the PAF1c recruits the BRE1-RAD6 E3 ubiquitin ligase complex to chromatin to promote monoubiquitination of H2BK120 (Kim et al., 2009; Kim and Roeder, 2009; Ng et al., 2003; Van Oss et al., 2016). The PAF1c is also necessary for deposition of H3K4me3 and H3K79me3 associated with transcriptionally active chromatin and linked with H2Bub (Dover et al., 2002; Kim and Roeder, 2009; Krogan et al., 2003; Nakanishi et al., 2009; Sun and Allis, 2002; Wood et al., 2003a, 2003b). Consistent with these data, our lab and others have shown that the PAF1 and CTR9 subunits of the complex make direct contact with the H3K4 methyltransferase MLL1 (Milne et al., 2010; Muntean et al., 2010).

Due to its direct interaction with MLL1, the PAF1c plays a central role in the pathogenesis of MLL-rearranged leukemia (Milne et al., 2010; Muntean et al., 2010). The interaction between the PAF1c and MLL fusion proteins is essential for activation of pro-leukemic targets such as *Hoxa9* and *Meis1* (Muntean et al., 2010, 2013). RNA expression

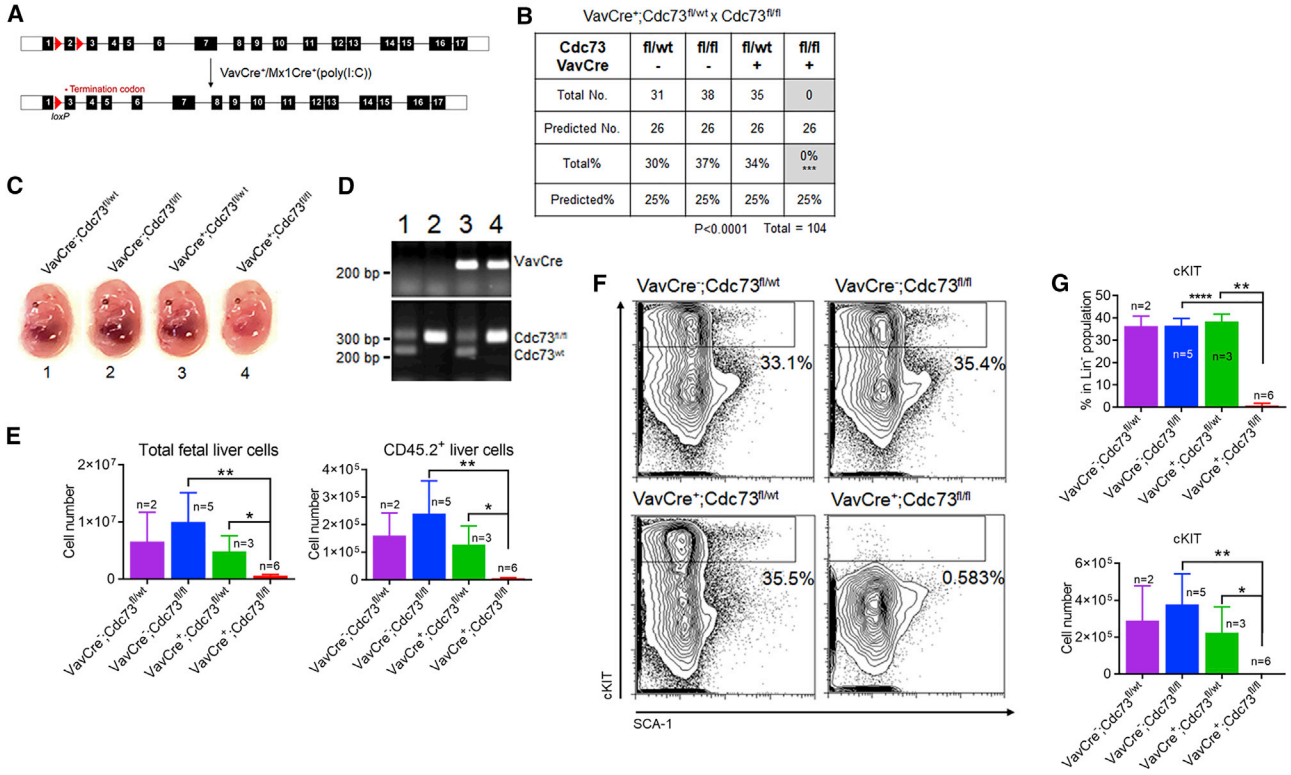

Figure 1. CDC73 Is Essential for Embryonic Hematopoiesis

(A) Graphical representation of the *Cdc73* gene containing *loxP* sites before and after Cre-mediated excision.

(B) Genotyping results from pups resulting from the indicated mating strategy.

(C) Representative images of embryonic day 14.5 (E14.5) embryos from mating strategy described in (B).

(D) Genotyping results from E14.5 numbered embryos shown in (C).

(E) Total number of liver cells and CD45.2$^+$ expressing cells in liver isolated from the indicated embryos.

(F) Representative flow cytometry plots showing Lin$^-$SCA-1$^+$cKIT$^+$ cell population in fetal liver.

(G) Quantification of the percentage (left) and total cell number (right) of cKIT$^+$ cells in the fetal liver of the indicated embryos.

*p < 0.05, **p < 0.01, ***p < 0.001, ****p < 0.0001. The p value was calculated using unpaired t test. See also Figure S1.

analyses show that knockout (KO) of the PAF1c subunit *Cdc73* in leukemic cells results in induction of a differentiation gene program in accordance with the differentiation and cell-cycle arrest observed in these cells (Serio et al., 2018). Importantly, targeted disruption of the PAF1c-MLL interaction specifically inhibits leukemic cell growth driven by MLL fusion proteins, but is tolerated by normal hematopoietic cells, signifying a cancer-specific function and potential therapeutic target (Muntean et al., 2013). Further, these data suggest that the PAF1c may control unique gene programs in normal versus malignant hematopoietic cells. These findings provide insights into the biomedical significance of the PAF1c in leukemia. However, the role of this multifunctional complex in normal hematopoietic development is still not clear. In this study, we evaluated the role of CDC73, a core component of the PAF1c (Kim et al., 2010; Rozenblatt-Rosen et al., 2005; Xu et al., 2017), in hematopoietic development and found that CDC73 is essential for hematopoietic stem cell (HSC) function. Interestingly, gene expression profiling demonstrates unique CDC73-mediated gene regulation in hematopoietic stem and progenitor cells (HSPCs) compared with AML cells, including *Hoxa9/Meis1* gene programs. These data point to disease-specific functions of CDC73 and the PAF1c that may be therapeutically targeted.

RESULTS

Loss of *Cdc73* Impairs Fetal Hematopoiesis

To understand the role of CDC73 during fetal hematopoiesis, we used VavCre mice, which express Cre and induce *loxP* recombination in fetal hematopoietic tissues (Gan et al., 2010). We crossed *Cdc73*$^{fl/fl}$ mice with *VavCre*$^{+/o}$; *Cdc73*$^{fl/wt}$ mice to induce excision of exon 2 of *Cdc73* generating a premature stop codon (Figure 1A). Henceforth,

hemizygous VavCre is referred to as VavCre$^+$. The frequency of the four predicted genotypes was monitored at birth by genotyping: *Cdc73$^{fl/wt}$*, *Cdc73$^{fl/fl}$*, *VavCre$^+$;Cdc73$^{fl/wt}$*, and *VavCre$^+$;Cdc73$^{fl/fl}$*. All 104 born pups were *VavCre$^+$;Cdc73$^{fl/wt}$*, *Cdc73$^{fl/wt}$*, or *Cdc73$^{fl/fl}$*, which differed markedly from the predicted Mendelian distribution (Figure 1B). The absence of *VavCre$^+$;Cdc73$^{fl/fl}$* pups suggests that VavCre-mediated *Cdc73* inactivation led to embryonic lethality. Thus, we performed timed mating and isolated embryonic day 14.5 embryos for analysis. Two breeding strategies were used to exclude the effect of VavCre activation in paternal germ cells: *VavCre$^+$;Cdc73$^{fl/wt}$*(♂) × *Cdc73$^{fl/fl}$*(♀) and *Cdc73$^{fl/fl}$*(♂) × *VavCre$^+$;Cdc73$^{fl/wt}$*(♀). With both breeding strategies, embryos with pale livers were observed (Figures 1C and S1), suggesting fetal hematopoietic failure. Genotyping revealed that embryos with pale livers were *VavCre$^+$;Cdc73$^{fl/fl}$*, while remaining embryos without an obvious phenotype were heterozygous for *Cdc73* or lacked *VavCre* (Figures 1D and S1). Six out of 16 embryos were *VavCre$^+$;Cdc73$^{fl/fl}$*, roughly matching the Mendelian distribution.

Next, we evaluated the hematopoietic defects of *VavCre$^+$;Cdc73$^{fl/fl}$*. Embryos with deleted *Cdc73* had significantly reduced fetal liver cellularity compared with *Cdc73$^{fl/wt}$* embryos and those lacking *VavCre* expression (Figure 1E). Flow cytometric analysis confirmed the loss of CD45.2$^+$ leukocytes in *VavCre$^+$;Cdc73$^{fl/fl}$* fetal livers (Figure 1E). These results suggested hematopoietic failure due to loss of *Cdc73*. Further, the percentage and total number of Lin$^-$cKIT$^+$ HSPCs were significantly reduced in the *VavCre$^+$;Cdc73$^{fl/fl}$* embryos (Figures 1F and 1G), while no difference was observed between *VavCre$^+$;Cdc73$^{fl/wt}$* embryos and *VavCre*-negative embryos (Figures 1F and 1G). Thus, we conclude that *Cdc73* is essential for the development and/or maintenance of fetal liver HSPCs.

CDC73 Is Essential for Adult Hematopoiesis and Indispensable for AML

Constitutive KO of *Cdc73* leads to embryonic lethality in mice (Wang et al., 2008). Thus, we used *Mx1Cre*-mediated conditional excision of *Cdc73* to study its role in adult hematopoiesis. *Mx1Cre* transgenic mice express Cre in bone marrow cells and other tissues in response to interferon, which is mimicked by polyinosinic:polycytidylic acid (poly(I:C)) administration (Kühn et al., 1995). *Mx1Cre$^{+/o}$;Cdc73$^{fl/fl}$* and *Mx1Cre$^{+/o}$;Cdc73$^{fl/wt}$* mice were generated to achieve inducible *Cdc73* allele deletion after poly(I:C) administration (Figure 1A). Henceforth, the hemizygous allele of *Mx1Cre* is referred to as *Mx1Cre$^+$*. *Mx1Cre$^+$* mice were used to test for potential Cre toxicity. To activate *Mx1Cre* expression, mice were treated with five doses of poly(I:C) (Figure 2A). Homozygous-deleted mice became moribund and had to be euthanized 11 to 16 days after poly(I:C) treatment. *Mx1Cre$^+$* and *Mx1Cre$^+$;Cdc73$^{fl/wt}$* mice showed no obvious sickness in the 2 months surveillance period (Figure 2B). Efficient *Cdc73* excision was achieved in *Mx1Cre$^+$;Cdc73$^{fl/wt}$* mice within 18 days and was still observed up to 64 days after poly(I:C) treatment (Figure 2C). *Cdc73* excision was achieved in *Mx1Cre$^+$;Cdc73$^{fl/fl}$* mice; however, a residual floxed *Cdc73* allele was detected (Figure 2C). We attribute this to near ablation of poly(I:C)-sensitive hematopoietic cells and the presence of poly(I:C)-insensitive bone marrow cells (Figure 2C, left panel). Further, poly(I:C) administration of *Cdc73$^{fl/fl}$* animals did not affect the excision or function of the *Cdc73* floxed allele (Figures 2C, right panel and S2A).

Morphological analysis of H&E-stained tibias from wild-type, heterozygous, and homozygous mice showed significant reduction in bone marrow cellularity in *Mx1Cre$^+$;Cdc73$^{fl/fl}$* mice (Figure 2D). In addition, the total number of bone marrow cells was significantly reduced in *Mx1Cre$^+$;Cdc73$^{fl/fl}$* mice compared with wild type and heterozygous mice (Figure 2E). As predicted from these data, peripheral blood profiling before and after homozygous excision showed that loss of *Cdc73* caused anemia and leukopenia compared with controls (Figures 2F, S2B, and S2C).

Previous reports demonstrated an essential function for the PAF1c in leukemogenesis *in vitro* (Milne et al., 2010; Muntean et al., 2013, 2010; Serio et al., 2018). We used the conditional Mx1Cre$^+$-*Cdc73* KO model to confirm a genetic requirement for *Cdc73* in MLL-AF9 leukemogenesis *in vivo*. Primary MLL-AF9-driven *Mx1Cre$^+$;Cdc73$^{fl/fl}$* leukemic cells were transplanted intravenously into sublethally irradiated mice followed by treatment with poly(I:C) or vehicle (Figure S2D). Vehicle-treated mice succumbed to leukemia within 25 days of transplantation. Excision of *Cdc73* led to a significant increase in disease latency compared with controls. Seven out of eight mice died at a median of 35.5 days due to leukemia, with one mouse not developing disease (Figure 2G). Importantly, genotyping of leukemic cells derived from poly(I:C)-treated mice showed retention of a floxed *Cdc73* allele, suggesting strong selective pressure against *Cdc73* excision in leukemic cells (Figure S2E). These data confirm a genetic requirement for *Cdc73* in both normal hematopoiesis and MLL-AF9-driven leukemia *in vivo*.

CDC73 Inactivation Is Deleterious to HSPCs

Acute anemia and leukopenia observed in our conditional knockout mouse model prompted us to investigate the effects of *Cdc73* loss on the hematopoietic stem and progenitor cell compartment. We isolated total bone marrow cells from *Mx1Cre$^+$*, *Mx1Cre$^+$;Cdc73$^{fl/wt}$*, and *Mx1Cre$^+$;Cdc73$^{fl/fl}$* mice when *Mx1Cre$^+$;Cdc73$^{fl/fl}$* appeared moribund and stained for HSPC markers (Lin$^-$SCA-1$^+$cKIT$^+$ [LSK]). Flow

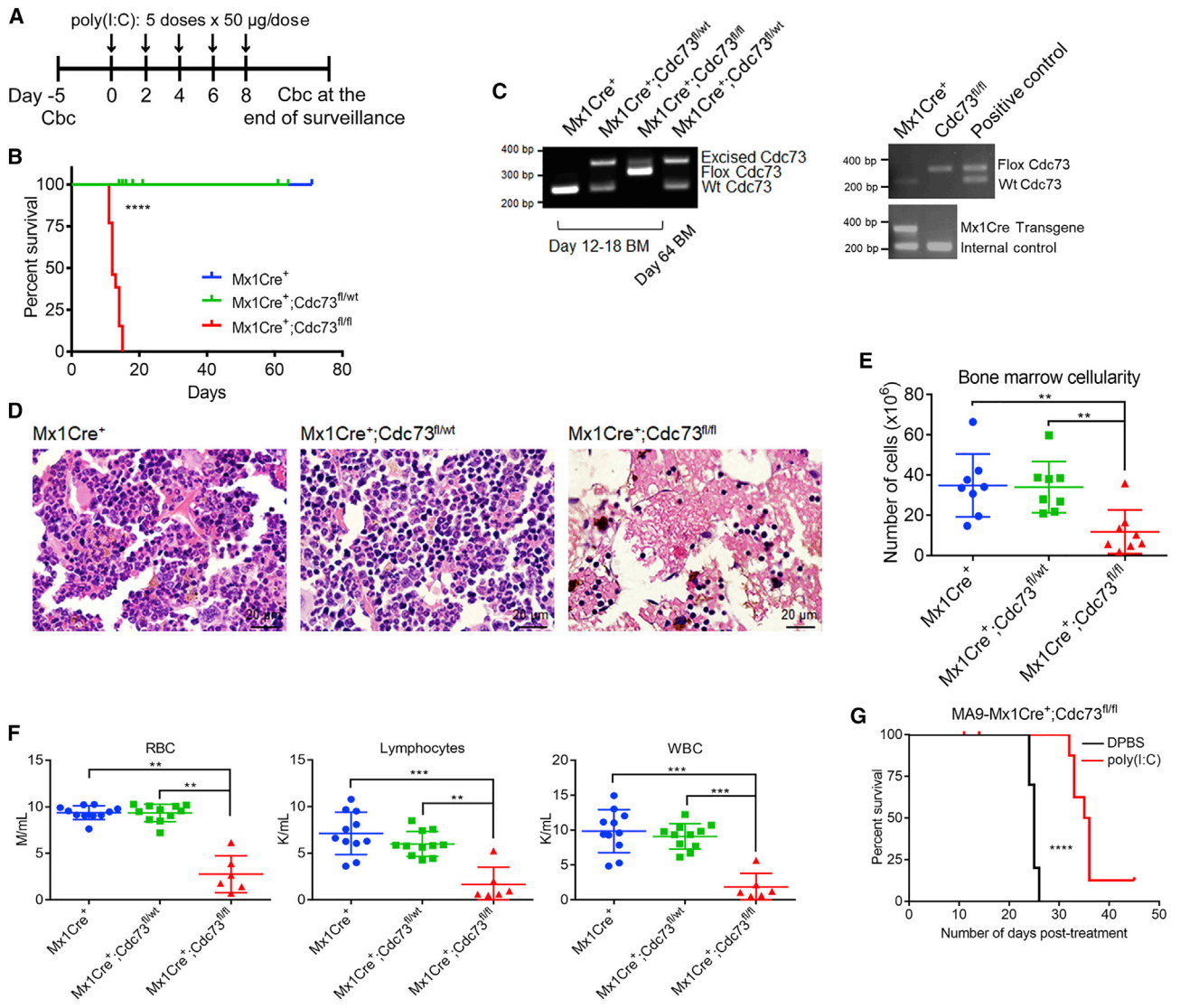

Figure 2. CDC73 Is Essential for Adult Hematopoiesis and MLL-AF9-Mediated Leukemogenesis

(A) Experimental protocol for poly(I:C) administration and Mx1Cre activation. Five doses of 50 µg poly(I:C) each were injected into mice intraperitoneally every other day. Complete blood count (CBC) was recorded at least 5 days before the first poly(I:C) injection and at the end of the surveillance time.

(B) Kaplan-Meier analysis of *Mx1Cre*$^{+}$ (blue, n = 11), *Mx1Cre*$^{+}$*;Cdc73*$^{fl/wt}$ (green, n = 11), and *Mx1Cre*$^{+}$*;Cdc73*$^{fl/fl}$ (red, n = 13) mice following poly(I:C) treatment. Censored points indicate mice were sacrificed for experimental purpose.

(C) Genotyping of total bone marrow cells demonstrating excision of floxed *Cdc73* in presence (left panel) or absence (right panel) of *Mx1Cre*$^{+}$ transgene. Positive control, *Cdc73*-specific genotypying was performed on DNA extracted from a *Cdc73*$^{fl/wt}$ mouse. BM, bone marrow.

(D) Representative image of H&E-stained cross-section of a tibia (100× magnification). Scale bars, 20 mm. Genotype is indicated at the top.

(E) Total number of bone marrow cells isolated from mice of indicated genotype following poly(I:C) treatment.

(F) Total number of red blood cells (RBC), lymphocyte, and white blood cells (WBC) from poly(I:C)-treated mice determined by CBC at moribund stage.

(G) Kaplan-Meier analysis of secondary MLL-AF9 leukemogenesis assay of mice transplanted with MA9-Mx1Cre^{+};Cdc73$^{fl/fl}$ cells. Mice were treated with poly(I:C) to excise *Cdc73* (n = 10) or DPBS as control (n = 10). Censored points indicate death not related to leukemia.

***p < 0.001, ****p < 0.0001 (Mantel-Cox test). Results of dot plots are represented as mean with SD (unpaired t test). See also Figure S2.

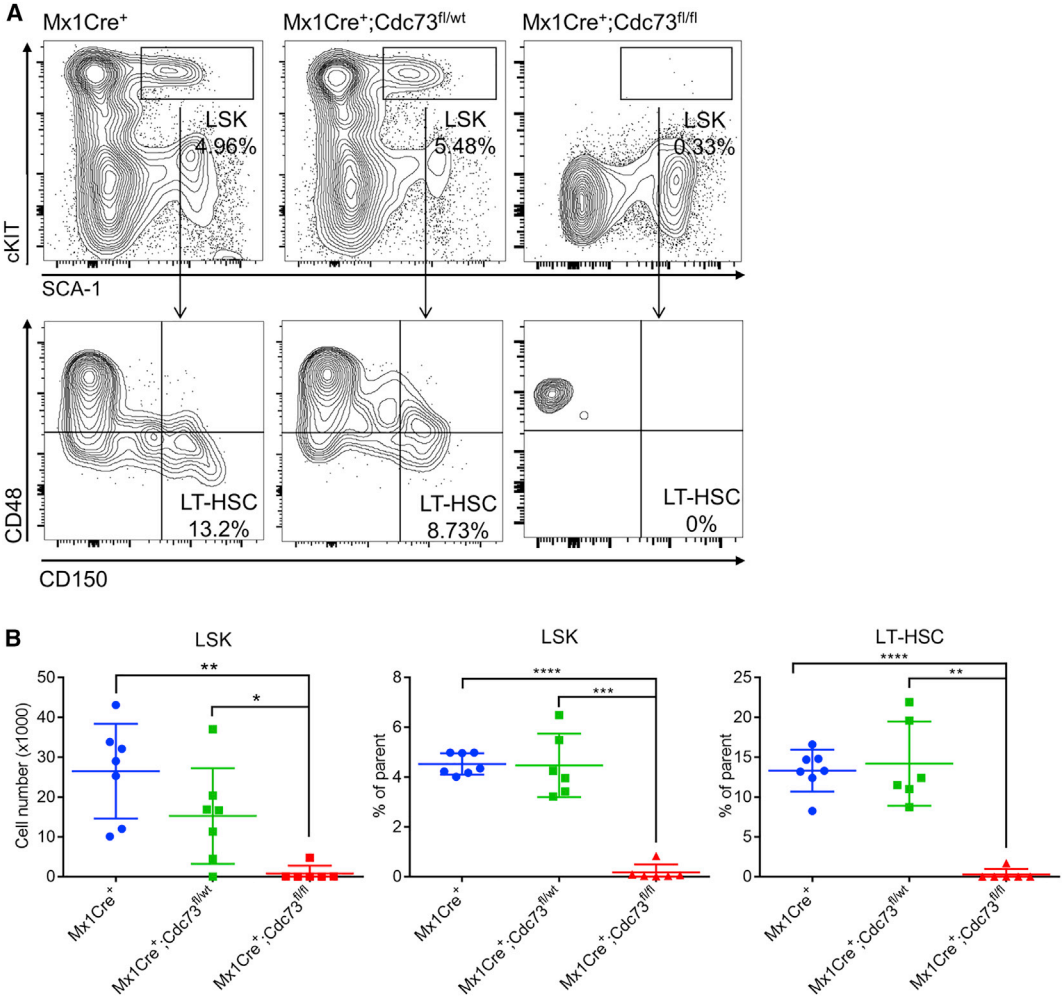

Figure 3. Loss of *Cdc73* Depletes HSPCs

(A) Representative flow plot showing the frequency of LSK (upper panel) and CD48$^-$CD150$^+$ (LT-HSC) (lower panel) cells in the bone marrow of *Mx1Cre*$^+$, *Mx1Cre*$^+$*;Cdc73*$^{fl/wt}$, and *Mx1Cre*$^+$*;Cdc73*$^{fl/fl}$ mice following poly(I:C) treatment.

(B) Compiled data for total LSKs (left), percent of LSKs (middle), and percent of LT-HSCs of LSK in the indicated mice ($n \geq 5$). *$p < 0.05$, ***$p < 0.001$, ****$p < 0.0001$. Results of dot plots are represented as mean with SD. Unpaired t test was used to calculate p value.

See also Figure S2.

cytometric analysis demonstrated that cKIT$^+$ cells were completely ablated on loss of *Cdc73*, while there was no effect on heterozygous or wild-type *Cdc73* cKIT$^+$ cells (Figures 3A and 3B). Staining for the SLAM-family proteins CD48 and CD150 in the LSK subset indicated a detrimental effect of *Cdc73* inactivation on long-term HSCs (CD150$^+$CD48$^-$ LT-HSCs), as well as on other progenitor subsets within the LSK compartment (Figure 3B). Additional analysis of myeloid, B cells, T cells, and erythroid progenitors also demonstrated a strong deleterious effect of *Cdc73* KO compared with controls (Figure S2F). These data suggest an essential function for CDC73 on bone marrow homeostasis.

A Cell-Autonomous Requirement for CDC73 in HSCs

To test for a cell-autonomous role for CDC73 in HSCs, we performed a non-competitive bone marrow transplantation assay. CD45.2$^+$ bone marrow cells isolated from *Mx1Cre*$^+$*;Cdc73*$^{fl/wt}$ and *Mx1Cre*$^+$*;Cdc73*$^{fl/fl}$ mice were transplanted into lethally irradiated CD45.1$^+$ recipient wild-type mice (Figure 4A). After allowing for engraftment and reconstitution of bone marrow for 7 weeks, CD45.1/2 chimerism was assessed by flow cytometric analysis on peripheral blood (Figure S3A). We administered five doses of poly(I:C) to excise the floxed *Cdc73* allele and monitored health (Figure 4B). Heterozygous mice expressing a single *Cdc73* allele showed no signs of illness and were normal

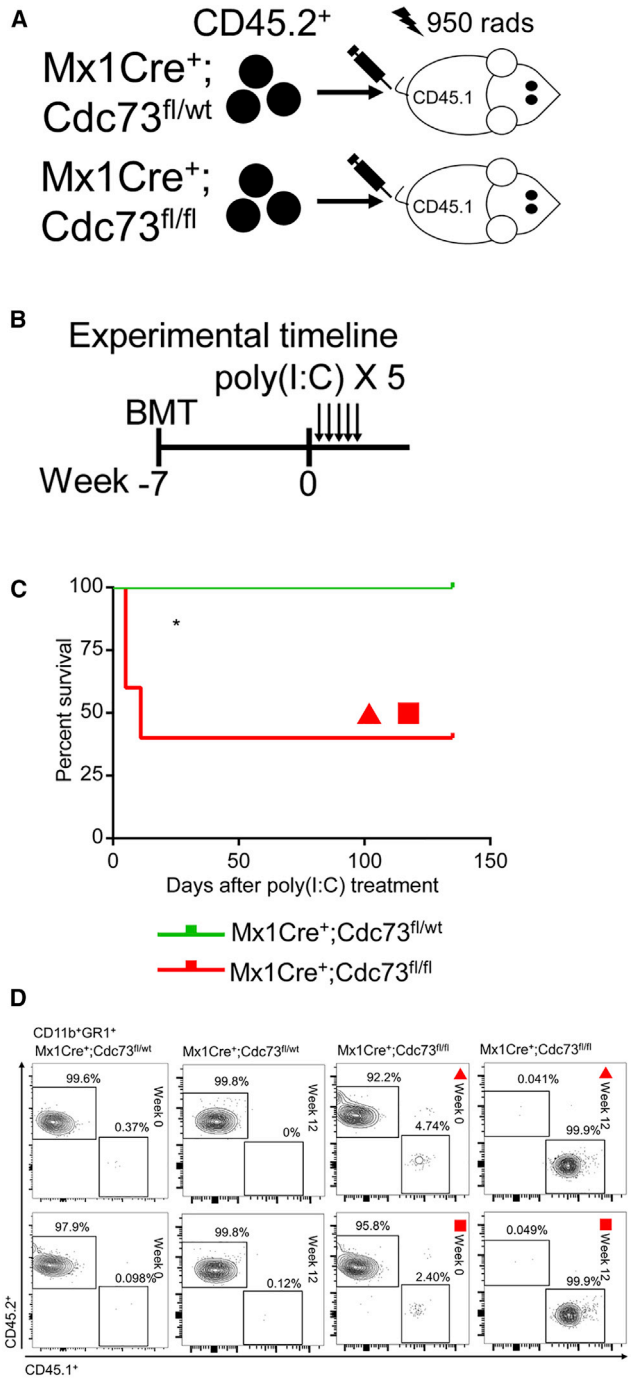

Figure 4. CDC73 Displays a Cell-Autonomous Role in HSCs

(A) Graphical representation of experimental strategy for non-competitive bone marrow transplantation assay. 5×10^5 bone marrow cells expressing the CD45.2$^+$ markers from *Mx1Cre*$^+$*;Cdc73*$^{fl/wt}$ (n = 5) and *Mx1Cre*$^+$*;Cdc73*$^{fl/fl}$ (n = 5) mice were transplanted into lethally irradiated wild-type (CD45.1$^+$) recipients.

(B) Experimental timeline of non-competitive bone marrow transplantation assay.

(C) Kaplan-Meier curve demonstrating the effect of conditional heterozygous or homozygous deletion of *Cdc73* in bone marrow cells.

(D) Flow plot showing the frequency of CD45.1$^+$- and CD45.2$^+$-expressing myeloid cells in peripheral blood of two *Mx1Cre*$^+$*;Cdc73*$^{fl/wt}$ mice and two *Mx1Cre*$^+$*;Cdc73*$^{fl/fl}$ surviving mice at week 0 and 12. The two surviving mice are depicted by red symbols marked in (C and D).

*$p < 0.05$. Statistics on survival curve was performed using Mantel-Cox test. See also Figure S3.

at the end of 135 days of surveillance (Figures 4C and S3B). Conversely, three out of five recipient mice that received bone marrow from *Mx1Cre*$^+$*;Cdc73*$^{fl/fl}$ donor died within 11 days (Figure 4C). The remaining two mice in this group survived throughout the period of surveillance (Figure 4C) with evidence of host CD45.1$^+$ bone marrow reconstitution (Figure 4D). Notably, our analysis demonstrated that less than 0.1% of peripheral blood myeloid cells were CD45.2$^+$, indicating efficient inactivation of the *Cdc73* gene (Figure 4D). In line with this interpretation, residual recipient-derived myeloid cells were detected before the initiation of poly(I:C) administration in these two mice (Figures 4D and S3A). Conversely, the peripheral blood of *Mx1Cre*$^+$*;Cdc73*$^{fl/wt}$ reconstituted mice was composed of CD45.2$^+$ donor cells, suggesting that heterozygous deletion of *Cdc73* did not affect the hematopoietic compartment (Figure 4D).

Next, we queried the role of CDC73 in the fitness of HSCs using a competitive bone marrow-reconstitution assay. CD45.2$^+$ donor cells from *Mx1Cre*$^+$, *Mx1Cre*$^+$*;Cdc73*$^{fl/wt}$, and *Mx1Cre*$^+$*;Cdc73*$^{fl/fl}$ mice were mixed and transplanted with equivalent CD45.1$^+$ wild-type competitor cells into lethally irradiated wild-type CD45.1$^+$ mice to generate bone marrow chimeras (Figure 5A). We allowed 7 weeks for engraftment and performed five injections of poly(I:C) to excise *Cdc73* as above (Figure 5B). Flow cytometry was performed on peripheral blood to assess the contribution of CD45.2$^+$ and CD45.1$^+$ cells to the myeloid, and B and T cell compartment at the indicated time points (Figure 5B). Within 2 weeks of poly(I:C) treatment, homozygous deletion of *Cdc73* resulted in a complete loss of CD45.2$^+$ myeloid cells (Figures 5C and 5D). We found a more gradual but significant depletion of CD45.2$^+$ cells within the B and T cell compartment in the peripheral blood following loss of *Cdc73* (Figure 5D). Notably, heterozygous deletion of *Cdc73* did not affect reconstituted bone marrow cells, suggesting that one allele of *Cdc73* was sufficient for hematopoiesis (Figures 5C and 5D). After 16 weeks, recipient animals were sacrificed, and bone marrow extracted to evaluate chimerism among HSCs (Figure 5B). The LT-HSC compartment was completely devoid of CD45.2$^+$ cells 16 weeks after homozygous deletion of *Cdc73* (Figure 5E).

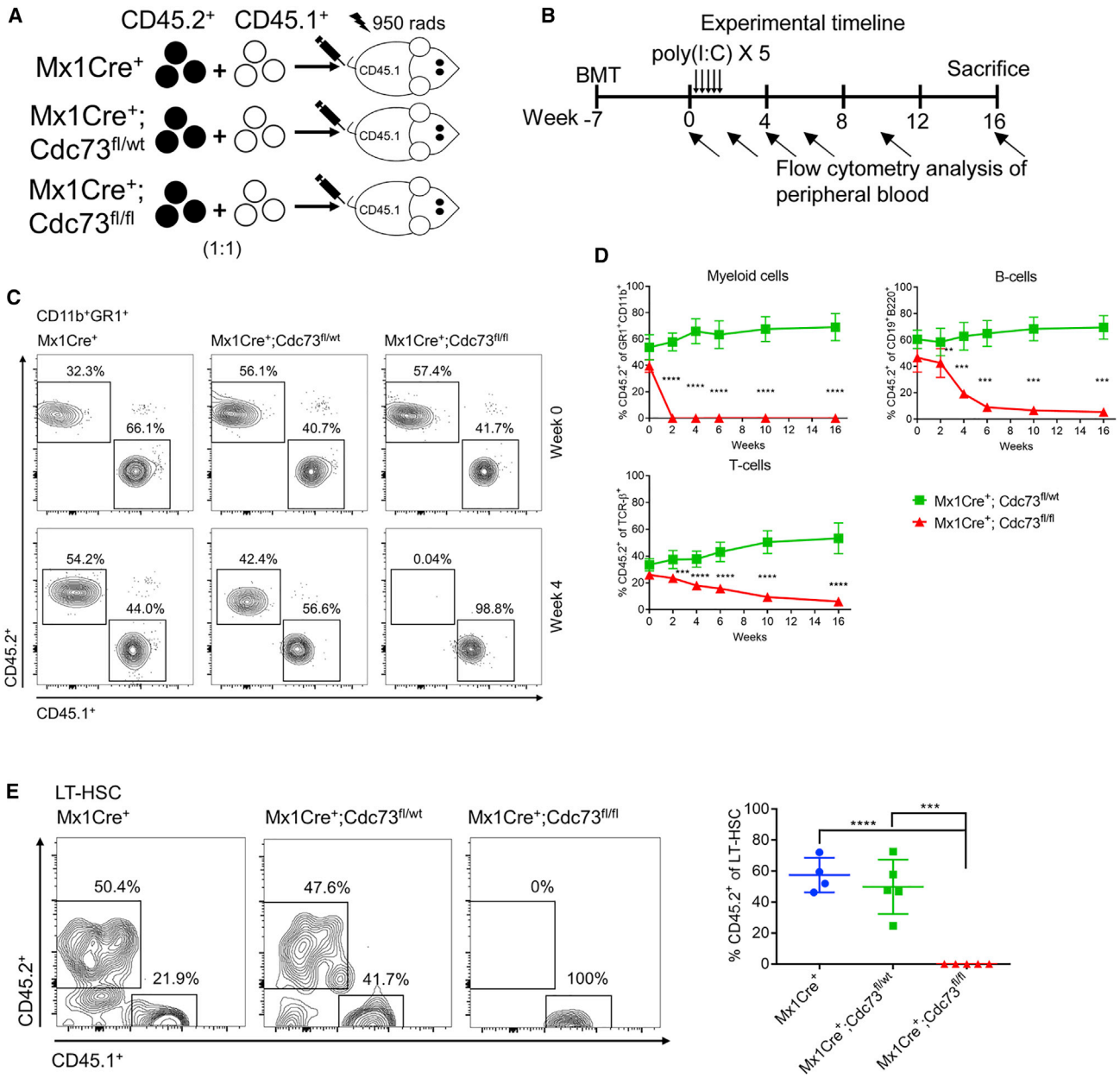

Figure 5. *Cdc73* Is Required for HSC Fitness

(A and B) Graphical representation of experimental strategy (A) and timeline (B) for competitive bone marrow transplant: bone marrow cells from *Mx1Cre*$^+$, *Mx1Cre*$^+$*;Cdc73*$^{fl/wt}$, and *Mx1Cre*$^+$*;Cdc73*$^{fl/fl}$ mice were mixed with wild-type cells (1:1) and transplanted into lethally irradiated CD45.1$^+$ recipient mice. Engraftment and reconstitution were allowed for 7 weeks followed by five doses of poly(I:C) injection. Contribution of CD45.2$^+$ (experimental) and CD45.1$^+$ (wild-type competitor) to peripheral blood was assessed using flow cytometry. After 16 weeks, mice were sacrificed and contribution of experimental and competitor cells to the HSC compartment was assessed by flow cytometry. *Mx1Cre*$^+$ (n = 5), *Mx1Cre*$^+$*;Cdc73*$^{fl/wt}$ (n = 10), and *Mx1Cre*$^+$*;Cdc73*$^{fl/fl}$ (n = 10).

(C) Frequency of CD45.2$^+$ and CD45.1$^+$ cells contributing to the myeloid (CD11b$^+$GR1$^+$) compartment at week 0 and after 4 weeks of poly(I:C) administration for *Mx1Cre*$^+$*;Cdc73*$^{fl/wt}$ and *Mx1Cre*$^+$*;Cdc73*$^{fl/fl}$ genotypes.

(D) Contribution of CD45.2$^+$ to the myeloid, B and T cell compartments in *Mx1Cre*$^+$*;Cdc73*$^{fl/fl}$ mice compared with *Mx1Cre*$^+$*;Cdc73*$^{fl/wt}$ mice following poly(I:C) treatment.

(legend continued on next page)

In contrast, wild-type and heterozygous CD45.2$^+$ cells contributed to the LT-HSC compartment as expected (Figure 5E). These results point to a cell-autonomous role for CDC73 in HSCs.

CDC73 Promotes Cell-Cycle Progression and Survival of HSPCs

We next aimed to understand the role of CDC73 in HSPCs. We performed a time course experiment to capture HSPCs after phenotypic changes associated with loss of *Cdc73* but before complete ablation of cKIT$^+$ cells. Our data indicate that HSPCs are progressively depleted with time following one poly(I:C) treatment (Figure S4A). *Cdc73* was efficiently excised in cKIT$^+$ cells 2 days after treatment with poly(I:C) (Figure S4B). Thus, to determine the function of CDC73 in HSPCs, we performed experiments 2 days after a single dose of poly(I:C).

Inducing *Cdc73* inactivation in the adult hematopoietic system caused complete disappearance of cKIT$^+$ HSPCs, as demonstrated above (Figure 3). To evaluate the effect of *Cdc73* KO on cell cycle, we analyzed cycling parameters in HSPCs from *Mx1Cre*$^+$ and *Mx1Cre*$^+$*;Cdc73*$^{fl/fl}$ mice following *Cdc73* excision. Mice were sacrificed 2 days after a single poly(I:C) injection, and bone marrow was collected for cell-cycle analysis by flow cytometry using KI67 (Figure 6A). We found a significant 2.5-fold increase in G0 cells, as well as decreased G1 and G2/S/M cells, following excision, suggesting a role for CDC73 in HSPC cell-cycle progression (Figure 6B).

Next, we investigated the apoptotic profile of HSPCs following *Cdc73* loss (Figure 6A). Flow cytometric analysis of cKIT$^+$ cells demonstrated that inactivation of *Cdc73* in HSPCs induced a significant increase in cells stained for both DAPI and Annexin V, demonstrating progression to late apoptosis and cell death. Concomitantly, our data demonstrate a modest reduction in the percentage of live cells (Annexin V$^-$; DAPI$^-$) in *Cdc73* excised cKIT$^+$ cells in comparison with control (Figure 6C).

To delineate the fate of *Cdc73* KO HSPCs, we studied bone marrow cells 48 h after loss of *Cdc73* resulting from a single dose of poly(I:C). We probed multipotent progenitors (MPPs) (LT-HSC, short-term HSC [ST-HSC], and MPPs) (Figure S5A), common lymphoid progenitors (CLPs) (Figure S5B), and myeloid progenitors (megakaryocyte-erythrocyte progenitor [MEPs], common myeloid progenitors [CMPs], and granulocyte-monocyte progenitors [GMPs]) (Figure S5C) by flow cytometry. Loss of *Cdc73* did not significantly affect the absolute number of LT-HSCs and ST-HSCs, however MPPs were reduced (Figure 6D). We observed a robust reduction in the absolute numbers of CLPs, MEPs, GMPs, and CMPs (Figures 6E and 6F). In the myeloid compartment, we observed increased numbers of CMPs undergoing apoptosis (Annexin V$^+$ and DAPI$^-$) (Figure 6G). We did not retrieve adequate number of cells to reliably test apoptosis in the LT-HSC, ST-HSC, MPP, and CLP populations. Given the reduction in several hematopoietic progenitor lineages, these data indicate a role for *Cdc73* in cell-cycle progression as well as survival of HSPCs and downstream progenitors.

CDC73 Regulates Similar and Distinct Genes in Normal and Malignant Hematopoiesis

To understand the molecular basis for the effects of *Cdc73* inactivation on HSPCs, we carried out transcriptome analysis. Total RNA was extracted from cKIT$^+$ cells from *Mx1Cre*$^+$*;Cdc73*$^{fl/fl}$ and *Mx1Cre*$^+$ mice 48 h after a single dose of poly(I:C). We found 433 genes to be repressed, while 390 genes were induced on *Cdc73* inactivation (1.5-fold; $p_{adj} < 0.05$) (Figure 7A; Table S1). Gene ontology indicated that *Cdc73* KO led to downregulation of immune response genes and genes involved in stress response. Conversely, *Cdc73* KO led to upregulation of cell-cycle gene programs and metabolic processes (Figure 7B) implicating CDC73 in various biological processes in HSPCs. Among the genes induced following *Cdc73* KO were those associated with cell cycle, specifically the cell-cycle inhibitors *p57* and *p21* (Figures 7A and 7C). By qRT-PCR, we confirmed a specific induction of *p57* and *p21*, but not *p27* on *Cdc73* inactivation (Figure 7C). Gene set analysis indicates that loss of *Cdc73* in HSPCs leads to enrichment of a cellular quiescence gene program (Figure 7D). By qRT-PCR, we confirmed that *Cdc73* KO led to upregulation of *Ptgs2* and *Cxcl10*, which play a role in cell-cycle arrest (Trifan et al., 1999; Yang et al., 2012) and *Nr4a2*, which is important for HSC quiescence (Figure 7D) (Sirin et al., 2010). In addition to the biological processes described above (Figure 7B), our data point to a role for CDC73 in regulating cell cycle in HSPCs consistent with the cell-cycle defect observed following excision of *Cdc73* (Figure 6). However, we cannot rule out transcriptome changes resulting from a relative enrichment of G0 cells due to apoptosis of non-G0 cells following loss of *Cdc73*.

Next, we compared the gene expression changes in HSPCs to those in MLL-AF9 leukemic cells following excision of *Cdc73* (Figure 7E) (Serio et al., 2018). Using a 1.5-fold change ($p_{adj} < 0.05$) cutoff, we found that 3,192

(E) Representative flow plot and quantification showing the contribution of CD45.1$^+$ and CD45.2$^+$ cells to LT-HSCs in *Mx1Cre*$^+$ (n = 5), *Mx1Cre*$^+$*;Cdc73*$^{fl/wt}$ (n = 5), and *Mx1Cre*$^+$*;Cdc73*$^{fl/fl}$ (n = 5) mice 16 weeks after poly(I:C) treatment.

**p < 0.01, ***p < 0.001, ****p < 0.0001. Results of plots are represented as mean with SD. Unpaired t test was used to calculate p value. See also Figure S3.

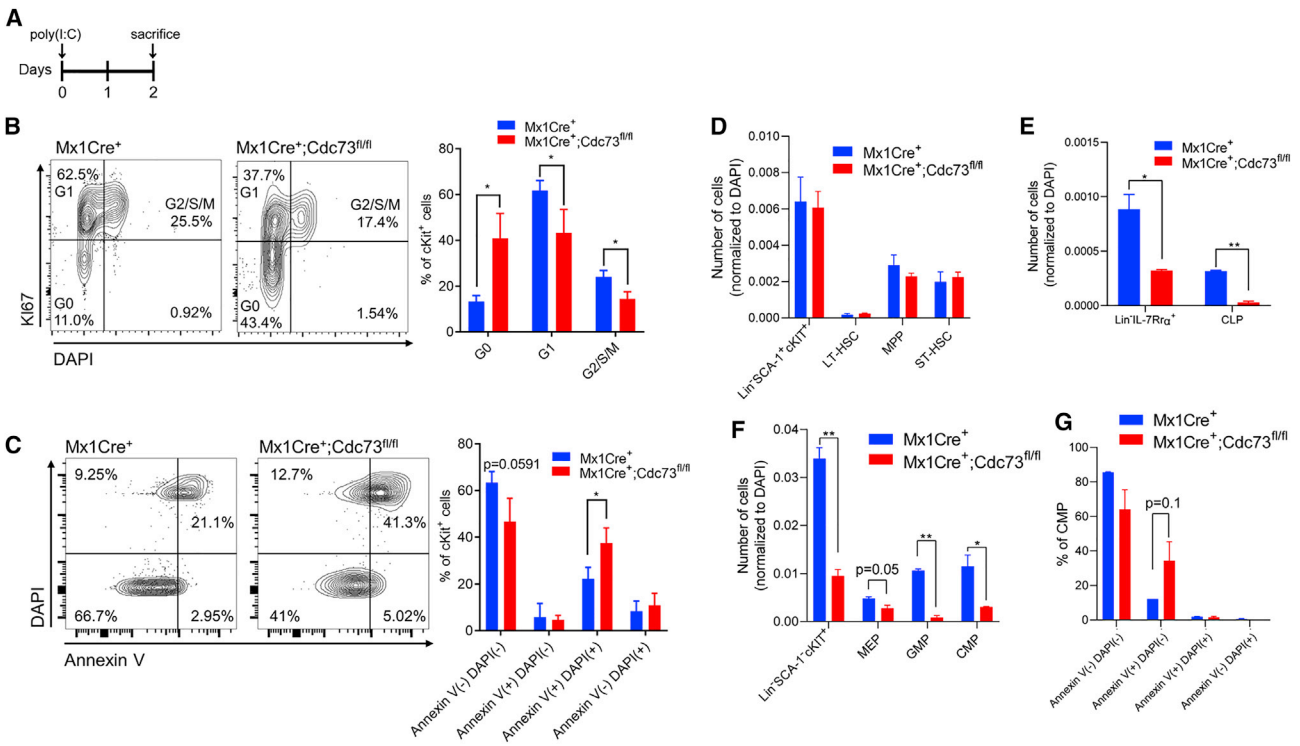

Figure 6. CDC73 Affects Cell Cycle and Apoptosis in HSPCs

(A) Experimental strategy and timeline: *Mx1Cre*$^{+}$ and *Mx1Cre*$^{+}$*;Cdc73*$^{fl/fl}$ mice were intraperitoneally injected with poly(I:C) (50 μg) as indicated. After 2 days, these mice were sacrificed to investigate cell cycle and apoptosis using KI67 or Annexin V and DAPI in cKIT^{+} cells.

(B) Representative flow cytometry plots showing the effect of *Cdc73* excision on the cell-cycle progression of cKIT^{+} cells (left). Bar graph shows quantitation of frequency of cells in G0, G1, and G2/S/M phase (n = 3) (right). Frequency is shown as a percentage of the parent population.

(C) Representative flow cytometry plot of apoptosis analysis following excision of *Cdc73* (left). Quantification of frequency of cKIT^{+} cells undergoing cell death with or without *Cdc73* (n = 3) (right).

(D–F) Quantification of absolute number of cells in hematopoietic stem and multipotent progenitor compartment (LT-HSC, ST-HSC, and MPP) (D), common lymphoid progenitors (CLPs) (E), and myeloid progenitors (MEPs, CMPs, and GMPs) (F). Total number of DAPI^{-} cells was used as the normalizing factor (n = 2).

(G) Frequency of CMPs undergoing cell death with or without *Cdc73* (n = 2).

*p < 0.05. The p value was calculated using unpaired t test. See also Figures S4 and S5.

genes are differentially expressed in leukemic cells compared with 823 genes in HSPCs (Figure 7E; Tables S1 and S2). Further, we found that CDC73 regulates both similar and distinct genes in leukemic cells and HSPCs. A total of 155 and 145 genes are commonly up- and downregulated, respectively, on loss of *Cdc73* in leukemic cells and HSPCs (Figure 7E; Table S2); and 1,690 and 240 genes are distinctly upregulated and 1,167 and 250 genes are distinctly downregulated in leukemic cells and HSPCs, respectively (Figure 7E; Table S2). These data point to unique gene-regulatory functions for CDC73 in normal and malignant hematopoiesis.

Next, we compared the gene programs controlled by CDC73 in leukemic cells and HSPCs. Loss of *Cdc73* in leukemic cells leads to downregulation of genes associated with early hematopoietic progenitors and upregulation of myeloid differentiation genes consistent with previous studies (Figures 7F and 7G) (Serio et al., 2018). Interestingly, while gene expression changes were observed within these gene programs following *Cdc73* inactivation in HSPCs there was not a concerted enrichment for either up- or downregulation (Figures 7F and 7G). Heatmap representation of gene expression changes within these gene programs clearly illustrates unique and differential transcriptional control by CDC73 between HSPCs and AML cells (Figures 7F and 7G; Table S3). Furthermore, our data indicate a similar effect on Hoxa9 gene targets. *Hoxa9* and the HOX cofactor *Meis1* are highly expressed in MLL-rearranged leukemia and are critical for leukemic transformation (Armstrong et al., 2002; Ayton and Cleary,

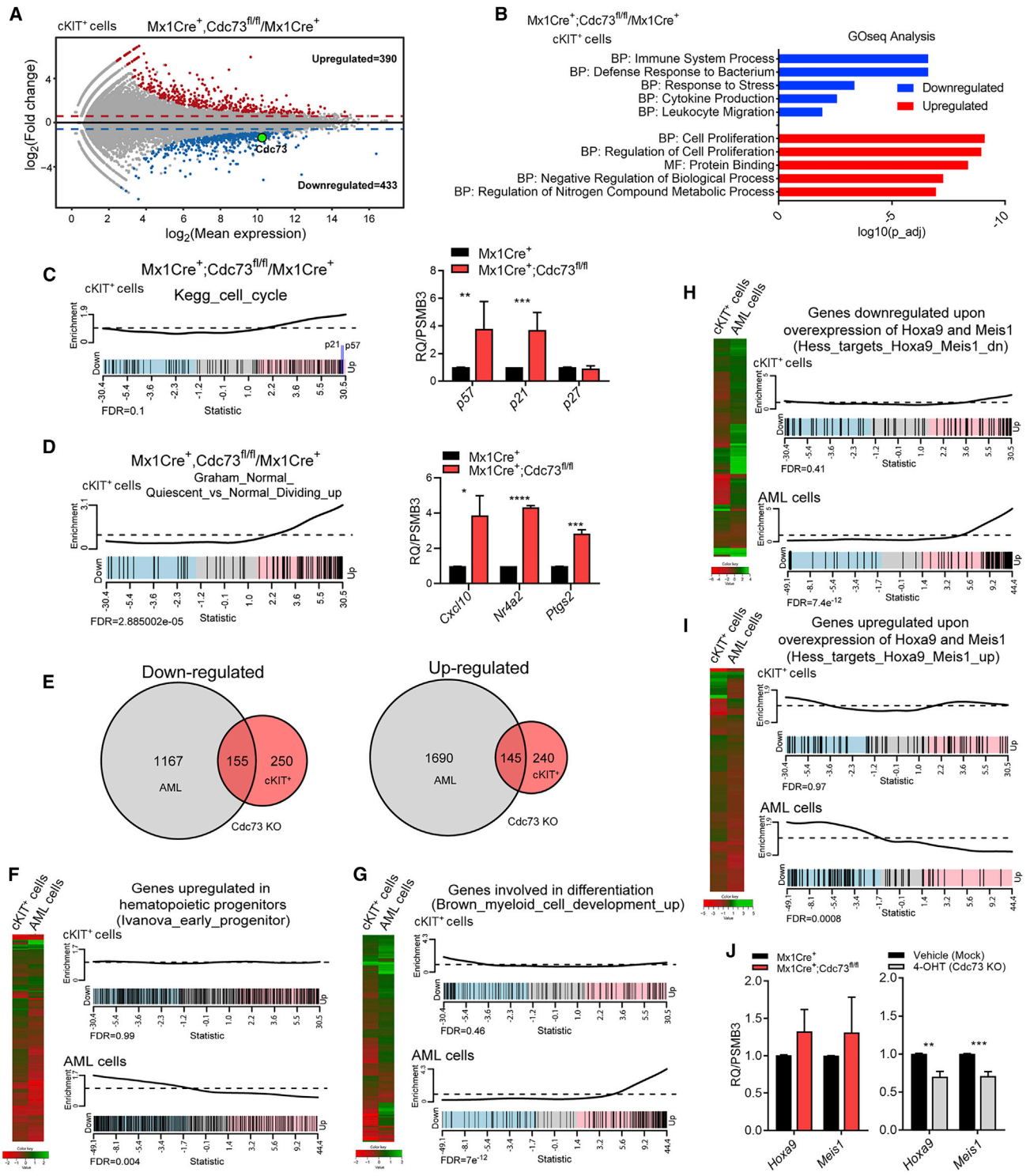

Figure 7. CDC73 Displays Unique Gene Regulatory Functions in Normal Hematopoiesis and AML

(A) The MA plot, which displays transformed log intensity ratios and log intensity average values, showing genome-wide differentially expressed genes (1.5-fold) in cKIT+ (HSPC) cells on *Cdc73* excision in three independent biological replicates. Red, significantly upregulated; blue, significantly downregulated. Significance was calculated based on adjusted p value.

(B) Gene ontology analysis shows cellular responses to *Cdc73* excision in HSPCs.

(legend continued on next page)

2003). The PAF1c is critically important for *Hoxa9* and *Meis1* expression in leukemic cells (Milne et al., 2010; Muntean et al., 2013; Serio et al., 2018). Consistent with these data, loss of *Cdc73* in MLL-AF9 AML cells leads to a significant downregulation of activated Hoxa9/Meis1 target genes and upregulation of Hoxa9/Meis1-repressed targets (Figures 7H and 7I). In contrast, excision of *Cdc73* in HSPCs again does not result in a concerted enrichment for either up- or downregulation of the Hoxa9/Meis1 gene programs, suggesting a context-specific role of the PAF1c (Figures 7H and 7I). Again, heatmap representation of expression changes suggests unique regulation of the *Hoxa9/Meis1* gene program by CDC73 in HSPCs and leukemic cells (Figures 7H and 7I; Table S3). Indeed, several clusters of genes display opposing transcriptional changes following loss of *Cdc73* in HSPCs compared with AML cells (Figures 7H and 7I; Table S3). We directly tested the effect of *Cdc73* deletion on the expression of *Hoxa9* and *Meis1* genes in MLL-AF9 leukemic cells and HSPCs. qRT-PCR analysis confirmed that loss of *Cdc73* reduced *Hoxa9* and *Meis1* expression in leukemic cells, consistent with our previous observations (Figure 7J) (Muntean et al., 2010, 2013; Ropa et al., 2018; Serio et al., 2018). In contrast and consistent with our RNA-seq data, *Cdc73* deletion in HSPCs led to no change or a modest increase in expression of *Hoxa9* and *Meis1*, respectively (Figure 7J). Mechanistically, differential gene regulation by CDC73 in HSPC and AML cells may reflect distinct epigenetic landscapes. For example, *CCR2* and *HOXA9*, which are directly bound by the PAF1c in leukemic cells (Figure S6B), are regulated in dissimilar ways by CDC73 in HSPCs and AML cells (Figures 7J and S6A). Consistent with this, THP1 leukemic cells display a clearly distinct epigenetic landscape of H3K4me3 and H3K79me2 at the *CCR2* and *HOXA9* locus compared with $CD34^+$ cells (Figure S6B). These data indicate differential roles and context-specific functions of the PAF1c subunit CDC73 in normal and malignant hematopoiesis.

DISCUSSION

Previous work from our laboratory and others has clearly demonstrated an essential role for the PAF1c, and specifically the CDC73 subunit, for AML cell proliferation (Milne et al., 2010; Muntean et al., 2010). In addition, we discovered that MLL-AF9 leukemic cells are more sensitive to disruption of the PAF1c-MLL interaction than normal hematopoietic cells (Muntean et al., 2013). While these studies point to leukemia-specific functions of the PAF1c that may be explored therapeutically, little was understood about the overall role of the PAF1c in normal hematopoietic development. In this study, we demonstrate an essential function of CDC73 in the murine hematopoietic system. Loss of *Cdc73*, specifically in hematopoietic cells, leads to hematopoietic failure and death in both fetuses and adult animals. CDC73 displayed cell-intrinsic functions for the survival and maintenance of HSCs (Figures 4 and 5). In $cKIT^+$ bone marrow cells, CDC73 controlled cell-cycle progression and survival (Figure 6). Importantly, we uncovered key differences in CDC73 gene program regulation between $cKIT^+$ hematopoietic cells and MLL-AF9 AML cells. These data provide evidence for differential function or regulation of CDC73 (and likely the PAF1c) in normal and malignant hematopoietic cells that necessitates further research.

Previous constitutive KO demonstrated a role for CDC73 in protecting cells from apoptosis in several tissues including liver, kidney, salivary glands, and others (Wang et al., 2008). Depletion of *Cdc73* in some solid tumors and normal cells induced cellular senescence, in part through the expression of *p21* (Jia et al., 2018). In AML cells, *Cdc73* excision causes reduced cell proliferation and myeloid differentiation (Serio et al., 2018). We observed a different role for the PAF1c in normal hematopoiesis in which loss of *Cdc73* in HSPCs leads to a mild cell-cycle defect with an upregulation of both *p21* and *p57* and increased cell death (Figure 6). Further work is necessary to determine the direct and indirect roles of

(C) Gene set analysis (GSA) shows upregulation of genes associated with cell-cycle processes on *Cdc73* excision. qRT-PCR verification of cell-cycle inhibitor genes identified in RNA-seq (n = 6).
(D) GSA analysis of genes upregulated in quiescent cells compared with normal dividing cells. qRT-PCR validation of *Cxcl10*, *Nr4a2*, and *Ptgs2* identified in this gene set (n = 3).
(E) Venn diagram showing the comparison of CDC73 differentially expressed genes in MLL-AF9 cells and HSPCs.
(F and G) GSA analysis and heatmap representation for an early hematopoietic progenitor gene program (F) and a myeloid differentiation program (G) following loss of *Cdc73* in MLL-AF9 cells and HSPCs.
(H and I) GSA analysis and heatmap representation for activated Hoxa9/Meis1 targets (H) and repressed Hoxa9/Meis1 targets (I) following loss of *Cdc73* in HSPCs and MLL-AF9 cells. Heatmaps represent gene expression changes of the corresponding gene set in HSPCs and AML cells following excision of *Cdc73* (F–I).
(J) qRT-PCR analysis of *Hoxa9* and *Meis1* on *Cdc73* excision in HSPCs (left, n = 3) and MLL-AF9 cells (right, n = 3).
Results are represented as mean with SD. *p < 0.05, **p < 0.01, ***p < 0.001, ****p < 0.0001. Unpaired t test was used to calculate p value. See also Figures S4 and S6 and Tables S1, S2 and S3.

the PAF1c that control cell-cycle progression in normal HSPCs.

Perhaps most notable from the current study was the difference in gene programs controlled by CDC73 in HSPCs and MLL-AF9 leukemic cells. Comparison of expression datasets obtained from HSPCs and MLL-AF9 leukemic cells before and after excision of *Cdc73* identified both unique and common gene expression changes (Figure 7). Direct comparisons of gene sets revealed that *Cdc73* excision in leukemic cells induces myeloid differentiation gene programs, which are not directionally enriched in normal HSPCs. We attribute this to differences in function or regulation of CDC73 and the PAF1c in normal and malignant hematopoiesis. In line with this, we observed a similar dichotomy in the regulation of a *Hoxa9/Meis1* gene program in leukemic cells compared with HSPCs (Figure 7). Interaction of the PAF1c with MLL fusion proteins is necessary for the expression of pro-leukemic genes *Hoxa9* and *Meis1* (Muntean et al., 2010, 2013). Indeed, excision of *Cdc73* from MLL-AF9 leukemic cells resulted in a downregulation of a *Hoxa9/Meis1* gene expression (Figure 7J) (Serio et al., 2018). In HSPCs, however, expression of *Hoxa9* and *Meis1* was unaltered or slightly upregulated on excision of *Cdc73* (Figure 7J), suggesting that CDC73 is not required for *Hoxa9* and *Meis1* expression in normal hematopoietic cells. This may be due to several possibilities. For example, it is possible that CDC73 and the PAF1c localize to *Hoxa9* and *Meis1* and operate to fine-tune expression in a temporal manner during differentiation. It is also possible that the PAF1c-MLL1 interaction may not be essential for targeting wild-type MLL1 and subsequent regulation of *Hoxa9* and *Meis1* in HSPCs, whereas the interaction is essential for MLL fusion protein recruitment. This prediction is supported by our previous work demonstrating that disruption of MLL-PAF1c interaction is tolerated during hematopoiesis (Muntean et al., 2013). Another possibility includes the epigenetic landscape at *Hoxa9* and *Meis1* in HSPCs. CDC73 and the PAF1c may regulate a different set or pattern of epigenetic modifications in HSPCs compared with MLL-AF9 leukemic cells, which are exquisitely sensitive to H3K4 and H3K79 methylation (Figure S6) (Bernt et al., 2011; Cao et al., 2014; Daigle et al., 2011; Thiel et al., 2010). Finally, it is interesting to consider differential posttranslational modifications of CDC73 in normal versus malignant hematopoiesis that may affect transcriptional targets. Further studies are required to better understand the observed differences in transcriptional regulation.

Here, we discovered an essential role for the PAF1c subunit, CDC73, in normal hematopoietic homeostasis. These data display similarities and differences with the role of MLL1 in normal hematopoiesis. Despite an essential role for MLL1 in hematopoietic development (Hess et al., 1997; Jude et al., 2007; McMahon et al., 2007; Yu et al., 1995), targeting the MLL1 H3K4 methyltransferase activity with a small-molecule inhibitor inhibits leukemic transformation without affecting bone marrow progenitor cells (Cao et al., 2014). Here, we observe significant differences in gene expression changes to the *Hoxa9/Meis1* program in normal versus leukemic cells following loss of *Cdc73*. This observation combined with our previous data showing increased sensitivity of MLL-AF9 leukemic cells, compared with normal hematopoiesis following disruption of the PAF1c-MLL1 (Muntean et al., 2013), suggests that novel small-molecule inhibitors to the PAF1-MLL1 interaction may be a useful therapeutic approach. Such an approach would specifically target leukemic functions of the PAF1c without disrupting all its functions. This study demonstrates the importance of gaining a thorough understanding of the role epigenetic regulators, such as the PAF1c, in both disease and normal states so that differences in function may be exploited for treatment purposes.

EXPERIMENTAL PROCEDURES

Mice

$Cdc73^{fl/fl}$ mice were backcrossed onto the C57Bl/6 background for ≥ 4 generations. $VavCre^{+}$ mice have been described (de Boer et al., 2003). $Mx1Cre^{+}$ (B6.Cg-Tg(Mx1-cre)1Cgn/J) mice were purchased from Jackson Laboratory and were bred at the University of Michigan's animal facilities. All experimental mice were bought from Taconic farms or Jackson Laboratory. $VavCre^{+};Cdc73^{fl/wt}$ mice of either gender were crossed to $Cdc73^{fl/fl}$ mice, and pups were genotyped using tail gDNA at postnatal day 10–14. All animal studies were approved by the University of Michigan's Committee on Use and Care of Animals and Unit for Laboratory Medicine.

Flow Cytometry

Antibodies for flow cytometry were purchased from BioLegend and Tonbo Biosciences and listed on Table S4. Details of staining procedures for flow cytometry analysis can be found in Supplemental Experimental Procedures.

Expression Analyses

Total RNA was extracted from sorted $Lin^{-}cKIT^{+}$ cells using the RNeasy Micro Kit (QIAGEN). Sequencing libraries were generated using the SMART-Seq v4 Ultra Low-Input RNA Kit (Takeda Biosciences) and single-end 50-bp mode was used for sequencing in HiSeq4000. RNA sequencing (RNA-seq) data on AML cells from Serio et al. (2018) was reanalyzed in this study. Details of bioinformatics analysis are described in Supplemental Experimental Procedures. Primers used for qRT-PCR analysis is listed in Table S5.

Raw RNA-seq data have been submitted to the GEO database (GSE117749) and can be requested from andrewmu@umich.edu. A full list of differentially expressed genes in HSPCs may be found in Supplemental Experimental Procedures available with the online version of this article.

Additional methods can be found in Supplemental Experimental Procedures.

SUPPLEMENTAL INFORMATION

Supplemental Information can be found online at https://doi.org/10.1016/j.stemcr.2019.03.010.

AUTHOR CONTRIBUTIONS

N.S. and L.C. contributed to the research design and acquired the data. N.S., L.C., H.H., and M.M. acquired the data. N.S., L.C., and A.G.M. analyzed the data. A.F. and I.M. provided critical technical assistance and guidance. J.R., N.S., and A.G.M. performed bioinformatic analyses. N.S. and A.G.M. drafted the manuscript. A.G.M. conceived the project and designed the research.

ACKNOWLEDGMENTS

We thank Drs. Mark Chiang, Daniel Lucas, Justin Serio, and Jean-Francois Rual for helpful discussions. This work was supported by an American Cancer Society Scholar Award RSG-15-046 (to A.G.M.), NIH grant T32CA140044 (to J.R.), NIH grant R01-AG-050509 (to I.M.), NIH grant R01-HL-136420 (to A.G.M.), and NIH award P30CA046592 to the University of Michigan Flow Core.

Received: October 9, 2018
Revised: March 25, 2019
Accepted: March 26, 2019
Published: April 25, 2019

REFERENCES

Armstrong, S.A., Staunton, J.E., Silverman, L.B., Pieters, R., den Boer, M.L., Minden, M.D., Sallan, S.E., Lander, E.S., Golub, T.R., and Korsmeyer, S.J. (2002). MLL translocations specify a distinct gene expression profile that distinguishes a unique leukemia. Nat. Genet. *30*, 41–47.

Ayton, P.M., and Cleary, M.L. (2003). Transformation of myeloid progenitors by MLL oncoproteins is dependent on Hoxa7 and Hoxa9. Genes Dev. *17*, 2298–2307.

Bernt, K.M., Zhu, N., Sinha, A.U., Vempati, S., Faber, J., Krivtsov, A.V., Feng, Z., Punt, N., Daigle, A., Bullinger, L., et al. (2011). MLL-rearranged leukemia is dependent on aberrant H3K79 methylation by DOT1L. Cancer Cell *20*, 66–78.

Cancer Genome Atlas Research Network, Ley, T.J., Miller, C., Ding, L., Raphael, B.J., Mungall, A.J., Robertson, A.G., Hoadley, K., Triche, T.J., Laird, P.W., et al. (2013). Genomic and epigenomic landscapes of adult de novo acute myeloid leukemia. N. Engl. J. Med. *368*, 2059–2074.

Cao, F., Townsend, E.C., Karatas, H., Xu, J., Li, L., Lee, S., Liu, L., Chen, Y., Ouillette, P., Zhu, J., et al. (2014). Targeting MLL1 H3K4 methyltransferase activity in mixed-lineage leukemia. Mol. Cell *53*, 247–261.

Carpten, J.D., Robbins, C.M., Villablanca, A., Forsberg, L., Presciuttini, S., Bailey-Wilson, J., Simonds, W.F., Gillanders, E.M., Kennedy, A.M., Chen, J.D., et al. (2002). HRPT2, encoding parafibromin, is mutated in hyperparathyroidism-jaw tumor syndrome. Nat. Genet. *32*, 676–680.

Chen, F.X., Woodfin, A.R., Gardini, A., Rickels, R.A., Marshall, S.A., Smith, E.R., Shiekhattar, R., and Shilatifard, A. (2015). PAF1, a molecular regulator of promoter-proximal pausing by RNA polymerase II. Cell *162*, 1003–1015.

Chen, F.X., Xie, P., Collings, C.K., Cao, K., Aoi, Y., Marshall, S.A., Rendleman, E.J., Ugarenko, M., Ozark, P.A., Zhang, A., et al. (2017). PAF1 regulation of promoter-proximal pause release via enhancer activation. Science *357*, 1294–1298.

Daigle, S.R., Olhava, E.J., Therkelsen, C.A., Majer, C.R., Sneeringer, C.J., Song, J., Johnston, L.D., Scott, M.P., Smith, J.J., Xiao, Y., et al. (2011). Selective killing of mixed lineage leukemia cells by a potent small-molecule DOT1L inhibitor. Cancer Cell *20*, 53–65.

de Boer, J., Williams, A., Skavdis, G., Harker, N., Coles, M., Tolaini, M., Norton, T., Williams, K., Roderick, K., Potocnik, A.J., et al. (2003). Transgenic mice with hematopoietic and lymphoid specific expression of Cre. Eur. J. Immunol. *33*, 314–325.

Dover, J., Schneider, J., Tawiah-Boateng, M.A., Wood, A., Dean, K., Johnston, M., and Shilatifard, A. (2002). Methylation of histone H3 by COMPASS requires ubiquitination of histone H2B by Rad6. J. Biol. Chem. *277*, 28368–28371.

Gan, T., Jude, C.D., Zaffuto, K., and Ernst, P. (2010). Developmentally induced Mll1 loss reveals defects in postnatal haematopoiesis. Leukemia *24*, 1732–1741.

Hanks, S., Perdeaux, E.R., Seal, S., Ruark, E., Mahamdallie, S.S., Murray, A., Ramsay, E., Del Vecchio Duarte, S., Zachariou, A., de Souza, B., et al. (2014). Germline mutations in the PAF1 complex gene CTR9 predispose to Wilms tumour. Nat. Commun. *5*, 4398.

He, N., Chan, C.K., Sobhian, B., Chou, S., Xue, Y., Liu, M., Alber, T., Benkirane, M., and Zhou, Q. (2011). Human polymerase-associated factor complex (PAFc) connects the super elongation complex (SEC) to RNA polymerase II on chromatin. Proc. Natl. Acad. Sci. U S A *108*, E636–E645.

Hess, J.L., Yu, B.D., Li, B., Hanson, R., and Korsmeyer, S.J. (1997). Defects in yolk sac hematopoiesis in Mll-null embryos. Blood *90*, 1799–1806.

Jaehning, J.A. (2010). The Paf1 complex: platform or player in RNA polymerase II transcription? Biochim. Biophys. Acta *1799*, 379–388.

Jia, Q., Nie, H., Wan, X., Fu, H., Yang, F., Li, Y., Wei, G., and Ni, T. (2018). Down-regulation of cancer-associated gene CDC73 contributes to cellular senescence. Biochem. Biophys. Res. Commun. *499*, 809–814.

Jude, C.D., Climer, L., Xu, D., Artinger, E., Fisher, J.K., and Ernst, P. (2007). Unique and independent roles for MLL in adult hematopoietic stem cells and progenitors. Cell Stem Cell *1*, 324–337.

Kim, J., and Roeder, R.G. (2009). Direct Bre1-Paf1 complex interactions and RING finger-independent Bre1-Rad6 interactions mediate histone H2B ubiquitylation in yeast. J. Biol. Chem. *284*, 20582–20592.

Kim, M., Ahn, S.-H., Krogan, N.J., Greenblatt, J.F., and Buratowski, S. (2004). Transitions in RNA polymerase II elongation complexes at the 3′ ends of genes. EMBO J. *23*, 354–364.

Kim, J., Guermah, M., McGinty, R.K., Lee, J.-S., Tang, Z., Milne, T.A., Shilatifard, A., Muir, T.W., and Roeder, R.G. (2009). RAD6-mediated transcription-coupled H2B ubiquitylation directly stimulates H3K4 methylation in human cells. Cell *137*, 459–471.

Kim, J., Guermah, M., and Roeder, R.G. (2010). The human PAF1 complex acts in chromatin transcription elongation both independently and cooperatively with SII/TFIIS. Cell *140*, 491–503.

Krogan, N.J., Dover, J., Wood, A., Schneider, J., Heidt, J., Boateng, M.A., Dean, K., Ryan, O.W., Golshani, A., Johnston, M., et al. (2003). The Paf1 complex is required for histone H3 methylation by COMPASS and Dot1p: linking transcriptional elongation to histone methylation. Mol. Cell *11*, 721–729.

Kühn, R., Schwenk, F., Aguet, M., and Rajewsky, K. (1995). Inducible gene targeting in mice. Science *269*, 1427–1429.

McMahon, K.A., Hiew, S.Y.-L., Hadjur, S., Veiga-Fernandes, H., Menzel, U., Price, A.J., Kioussis, D., Williams, O., and Brady, H.J.M. (2007). Mll has a critical role in fetal and adult hematopoietic stem cell self-renewal. Cell Stem Cell *1*, 338–345.

Milne, T.A., Kim, J., Wang, G.G., Stadler, S.C., Basrur, V., Whitcomb, S.J., Wang, Z., Ruthenburg, A.J., Elenitoba-Johnson, K.S.J., Roeder, R.G., et al. (2010). Multiple interactions recruit MLL1 and MLL1 fusion proteins to the HOXA9 locus in leukemogenesis. Mol. Cell *38*, 853–863.

Moniaux, N., Nemos, C., Schmied, B.M., Chauhan, S.C., Deb, S., Morikane, K., Choudhury, A., Vanlith, M., Sutherlin, M., Sikela, J.M., et al. (2006). The human homologue of the RNA polymerase II-associated factor 1 (hPaf1), localized on the 19q13 amplicon, is associated with tumorigenesis. Oncogene *25*, 3247–3257.

Mueller, C.L., and Jaehning, J.A. (2002). Ctr9, Rtf1, and Leo1 are components of the Paf1/RNA polymerase II complex. Mol. Cell. Biol. *22*, 1971–1980.

Mueller, J.E., Canze, M., and Bryk, M. (2006). The requirements for COMPASS and Paf1 in transcriptional silencing and methylation of histone H3 in *Saccharomyces cerevisiae*. Genetics *173*, 557–567.

Muntean, A.G., Tan, J., Sitwala, K., Huang, Y., Bronstein, J., Connelly, J.A., Basrur, V., Elenitoba-Johnson, K.S.J., and Hess, J.L. (2010). The PAF complex synergizes with MLL fusion proteins at HOX loci to promote leukemogenesis. Cancer Cell *17*, 609–621.

Muntean, A.G., Chen, W., Jones, M., Granowicz, E.M., Maillard, I., and Hess, J.L. (2013). MLL fusion protein-driven AML is selectively inhibited by targeted disruption of the MLL-PAFc interaction. Blood *122*, 1914–1922.

Nakanishi, S., Lee, J.S., Gardner, K.E., Gardner, J.M., Takahashi, Y., Chandrasekharan, M.B., Sun, Z.-W., Osley, M.A., Strahl, B.D., Jaspersen, S.L., et al. (2009). Histone H2BK123 monoubiquitination is the critical determinant for H3K4 and H3K79 trimethylation by COMPASS and Dot1. J. Cell Biol. *186*, 371–377.

Ng, H.H., Dole, S., and Struhl, K. (2003). The Rtf1 component of the Paf1 transcriptional elongation complex is required for ubiquitination of histone H2B. J. Biol. Chem. *278*, 33625–33628.

Pavri, R., Zhu, B., Li, G., Trojer, P., Mandal, S., Shilatifard, A., and Reinberg, D. (2006). Histone H2B monoubiquitination functions cooperatively with FACT to regulate elongation by RNA polymerase II. Cell *125*, 703–717.

Qiu, H., Hu, C., Wong, C.-M., and Hinnebusch, A.G. (2006). The Spt4p subunit of yeast DSIF stimulates association of the Paf1 complex with elongating RNA polymerase II. Mol. Cell. Biol. *26*, 3135–3148.

Ropa, J., Saha, N., Chen, Z., Serio, J., Chen, W., Mellacheruvu, D., Zhao, L., Basrur, V., Nesvizhskii, A.I., and Muntean, A.G. (2018). PAF1 complex interactions with SETDB1 mediate promoter H3K9 methylation and transcriptional repression of Hoxa9 and Meis1 in acute myeloid leukemia. Oncotarget *9*, 22123–22136.

Rozenblatt-Rosen, O., Hughes, C.M., Nannepaga, S.J., Shanmugam, K.S., Copeland, T.D., Guszczynski, T., Resau, J.H., and Meyerson, M. (2005). The parafibromin tumor suppressor protein is part of a human Paf1 complex. Mol. Cell. Biol. *25*, 612–620.

Serio, J., Ropa, J., Chen, W., Mysliwski, M., Saha, N., Chen, L., Wang, J., Miao, H., Cierpicki, T., Grembecka, J., et al. (2018). The PAF complex regulation of Prmt5 facilitates the progression and maintenance of MLL fusion leukemia. Oncogene *37*, 450–460.

Sirin, O., Lukov, G.L., Mao, R., Conneely, O.M., and Goodell, M.A. (2010). The orphan nuclear receptor Nurr1 restricts the proliferation of haematopoietic stem cells. Nat. Cell Biol. *12*, 1213–1219.

Sun, Z.-W., and Allis, C.D. (2002). Ubiquitination of histone H2B regulates H3 methylation and gene silencing in yeast. Nature *418*, 104–108.

Thiel, A.T., Blessington, P., Zou, T., Feather, D., Wu, X., Yan, J., Zhang, H., Liu, Z., Ernst, P., Koretzky, G.A., et al. (2010). MLL-AF9-induced leukemogenesis requires coexpression of the wild-type Mll allele. Cancer Cell *17*, 148–159.

Tomson, B.N., and Arndt, K.M. (2013). The many roles of the conserved eukaryotic Paf1 complex in regulating transcription, histone modifications, and disease states. Biochim. Biophys. Acta *1829*, 116–126.

Trifan, O.C., Smith, R.M., Thompson, B.D., and Hla, T. (1999). Overexpression of cyclooxygenase-2 induces cell cycle arrest. Evidence for a prostaglandin-independent mechanism. J. Biol. Chem. *274*, 34141–34147.

Van Oss, S.B., Shirra, M.K., Bataille, A.R., Wier, A.D., Yen, K., Vinayachandran, V., Byeon, I.-J.L., Cucinotta, C.E., Héroux, A., Jeon, J., et al. (2016). The histone modification domain of Paf1 complex subunit Rtf1 directly stimulates H2B ubiquitylation through an interaction with Rad6. Mol. Cell *64*, 815–825.

Van Oss, S.B., Cucinotta, C.E., and Arndt, K.M. (2017). Emerging insights into the roles of the Paf1 complex in gene regulation. Trends Biochem. Sci. *42*, 788–798.

Wade, P.A., Werel, W., Fentzke, R.C., Thompson, N.E., Leykam, J.F., Burgess, R.R., Jaehning, J.A., and Burton, Z.F. (1996). A novel collection of accessory factors associated with yeast RNA polymerase II. Protein Expr. Purif. *8*, 85–90.

Wang, P., Bowl, M.R., Bender, S., Peng, J., Farber, L., Chen, J., Ali, A., Zhang, Z., Alberts, A.S., Thakker, R.V., et al. (2008). Parafibromin, a component of the human PAF complex, regulates growth factors and is required for embryonic development and survival in adult mice. Mol. Cell. Biol. *28*, 2930–2940.

Wood, A., Krogan, N.J., Dover, J., Schneider, J., Heidt, J., Boateng, M.A., Dean, K., Golshani, A., Zhang, Y., Greenblatt, J.F., et al. (2003a). Bre1, an E3 ubiquitin ligase required for recruitment and substrate selection of Rad6 at a promoter. Mol. Cell *11*, 267–274.

Wood, A., Schneider, J., Dover, J., Johnston, M., and Shilatifard, A. (2003b). The Paf1 complex is essential for histone

monoubiquitination by the Rad6-Bre1 complex, which signals for histone methylation by COMPASS and Dot1p. J. Biol. Chem. *278*, 34739–34742.

Xu, Y., Bernecky, C., Lee, C.-T., Maier, K.C., Schwalb, B., Tegunov, D., Plitzko, J.M., Urlaub, H., and Cramer, P. (2017). Architecture of the RNA polymerase II-Paf1C-TFIIS transcription elongation complex. Nat. Commun. *8*, 15741.

Yang, L.-L., Wang, B.-Q., Chen, L.-L., Luo, H.-Q., and Wu, J.-B. (2012). CXCL10 enhances radiotherapy effects in HeLa cells through cell cycle redistribution. Oncol. Lett. *3*, 383–386.

Yu, B.D., Hess, J.L., Horning, S.E., Brown, G.A., and Korsmeyer, S.J. (1995). Altered Hox expression and segmental identity in Mll-mutant mice. Nature *378*, 505–508.

Yu, M., Yang, W., Ni, T., Tang, Z., Nakadai, T., Zhu, J., and Roeder, R.G. (2015). RNA polymerase II-associated factor 1 regulates the release and phosphorylation of paused RNA polymerase II. Science *350*, 1383–1386.

Zeng, H., and Xu, W. (2015). Ctr9, a key subunit of PAFc, affects global estrogen signaling and drives ERα-positive breast tumorigenesis. Genes Dev. *29*, 2153–2167.